# Testing and Design of Longitudinal Reinforcement for Cantilevered Bridge Piers

BORIS S. BROWZIN

**Deep cantilever specimens representing cantilevered bridge piers were tested for the purpose of studying their structural behavior. It has been established that the strength of the tested specimens is substantially superior to the strength predicted by conventional analysis. A new design method has been proposed for longitudinal reinforcement based on principles of static equilibrium with parameters derived from testing. The shear strength of specimens was substantially greater than was anticipated from the design. An example is provided to demonstrate the proposed design method, which provides a substantial reduction in the longitudinal reinforcement of bridge pier cantilevers.**

A double cantilever system consisting of deep cantilevers at the top of bridge piers, supporting the deck, is a rational approach that leads to substantial savings in bridge construction, particularly for highly elevated intersections or deep valley crossings. The double cantilever system made it possible to build a single central pier as a replacement for the older design in which two supporting piers were used. Despite the rationality of using central piers with double cantilevers at the top, there is no research evidence on the behavior of deep double cantilevers.

Deep double cantilevers are also used to support precast beams at the top of columns or for footings.

A characteristic of deep cantilevers is a large depth-to-span ratio--say, larger than one. Other structural elements with large depth-to-span ratios are brackets (corbels) and deep beams.

The geometry of deep structural elements influences the behavior of the element. For example, brackets in most tests fail because of cracks that develop from the point of stress concentration at the intersection of the upper horizontal surface of the bracket with the vertical surface of the column face, whereas most bridge pier cantilever specimens fail because of a crack that starts at the point where the concentrated load is applied to the specimen. Therefore, design methods for deep bridge cantilevers must be different from those used in the design of brackets.

This paper is based on tests of deep double cantilever specimens. The tests are described first. Test results are used to establish a new approach for analysis and design of longitudinal reinforcement. Based on the principle of static equilibrium and test results, it has been found that the needed amount of longitudinal reinforcement is substantially smaller than that resulting from a conventional analysis. It was also observed that the shear strength of the specimens was substantially higher than is usually assumed. Consequently, the shear stresses are not governing design criteria, and shear reinforcement, depending on the slope of the bottom face, may not be required. Other design aspects of deep cantilevers, such as anchorage of longitudinal bars and temperature reinforcement, were not considered in this testing program. The conventional design practice appears adequate, particularly for anchorage. Previous work on deep structural elements has consisted of testing deep beams and brackets (corbels). Work on deep beams is not reported in this paper because the structural behavior of deep beams differs from that of deep cantilevers. The work on brackets is summarized below.

Corbels were extensively investigated in Portland Cement Association (PCA) laboratories by Kriz and Raths (1). The PCA tests resulted in empirical equations based on statistical results from tests. It is regrettable that the principles of statics were neglected in the research of Kriz and Raths. Other works on corbels are listed in a report by the American Society of Civil Engineers (ASCE) (2), among them works by Mehmel and Beckner, Mehmel and Freitag, and Commissie and others. The investigation of corbels by Niedenhoff (3) and Franz and Niedenhoff (4) resulted in new information on the mechanisms of corbel behavior. Publications oriented toward establishing a design method for corbels based on "satisfaction of the laws of statics" are reported by Mattock, Chen, and Soongswang (5) and Mattock (6). According to the best evidence available to me, cantilevers of the geometry described in this paper have never been tested.

The following sections of this paper provide the description of the experimental setup, resulting load-stress characteristics, the analysis and design of reinforcement with design examples, and a tentative analysis of the stress distribution in a cross section of a cantilever.

Because a considerable amount of effort was applied in order to achieve a careful setup of testing and measurements, it is considered appropriate to provide a detailed account of the test results in this paper. Furthermore, since these tests were used in establishing a new approach for the design and analysis of an important structural element in the development of the national transportation system--i.e., bridge piers with cantilevers--it is believed that the experimental data base presented in detail will substantiate and justify the proposed approach.

## NOTATION

The following notation is used in this paper:

- $A_s$ = cross-sectional area of reinforcement;
- $a$ = "shear span," distance from the point of application of the load to the cross section considered;
- $b$ = width of the cross section;
- $C$ = resultant of normal stresses in concrete at a given cross section;
- $d$ = depth of the cross section;
- $f'_c$ = specified compressive strength of concrete;
- $f_s$ = stress in reinforcement;
- $f_{su}$ = stress in reinforcement at failure;
- $f_y$ = yielding stress in reinforcement;
- $j$ = parameter determining the location of the resultant of concrete compressive stresses in a cross section above the centroid of reinforcement;
- $j_F$ = magnitude of the parameter j at failure;
- $T$ = resultant of tensile stresses in reinforcement;
- $V$ = reaction at tested specimens, load on cantilevers;
- $2V$ = load on tested specimens;
- $V_u$ = V at failure;
- $2V_u$ = 2V at failure; and
- $\rho$ = ratio of reinforcement or percentage of reinforcement.

## EXPERIMENTAL SETUP AND TESTING

Experimental work was conducted at the National Bureau of Standards (specimens N1 and N2) and at Case Institute of Technology (specimens C1, C2, C3, C4, and C5). An arbitrary shape was selected for the specimens, which were tested in the upside-down position (see Figure 1). The overall dimensions of the specimens were 36x25.5x12 in (91.4x64.8x30.5 cm). The span between the supports was 27 in (68.6 cm). Axes numbered 1 through 15 were used to identify cross sections of the specimens (see Figure 2). Axes 1, 3, 5, and 7 were separated by 5 in (12.7 cm) as were axes 9, 11, 13, and 15. The specimens rested on 1x4x12-in (2.5x10.2x30.5-cm) supporting plates, which in turn rested on rollers at each side of the span. For specimens C1-C5, two rollers in contact were used at each support as a precaution against possible escape of the rollers under loading action. Specimens N1 and N2 were tested with one roller welded at support A and one free roller at support B, as shown in Figure 2.

The concrete used was Type III, which had a specified strength of 3000 psi (20.7 MPa); the strengths actually obtained ranged from 3930 to 5950 psi (27.1-41.0 MPa) and the moduli of elasticity ranged from 3.1 million to 4.8 million psi (21 400-33 100 MPa) (see Table 1).

The characteristics of the reinforcing steel in the N and C specimens were as follows:

| Specimen Type | Yield Point (psi 000s) | Ultimate Strength (psi 000s) | Elastic Modulus (psi 000 000s) |
|---|---|---|---|
| N | 45.3 | 74 | 26 |
| C | 45 | 77 | 29 |

The cross-sectional area of the reinforcement of specimens N1 and C1 was designed to provide a reinforcement ratio at the middle of the specimen, axis 8, that would approximately correspond to allowable stresses, $f_s$ = 20 000 psi (138 MPa) and $f_c$ = 1350 psi (9.3 MPa), at working load in steel and concrete, respectively. Normal practice was followed to obtain an approximation of 21 in (53.3 cm) for the depth of the cross-sectional area at axis 8. The distance from the bottom of the specimens to the centroid of the reinforcement was 1.5 in (3.8 cm). Specimens N1 and C1 were reinforced by two layers of bars, the others by one layer. The rein-

Figure 1. Sectional view of specimens.

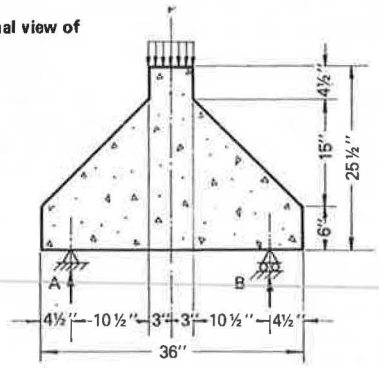


Figure 2. Structural details of specimens N1 and N2, including grid system and location of strain gages.

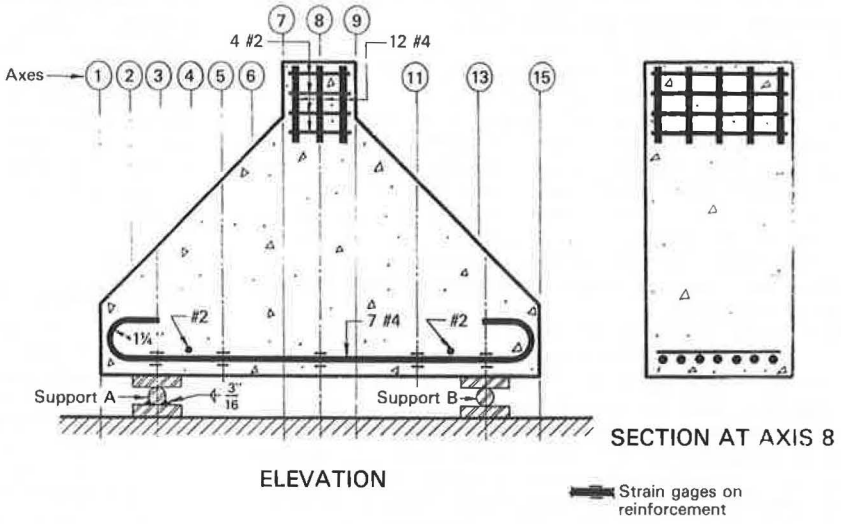


Table 1. Characteristics of specimens.

| Specimen | Ultimate Strength of Concrete (psi) | Modulus of Elasticity of Concrete (psi 000 000s) | Bars | | Area of Reinforcement ($in^2$) | Reinforcement Ratio at Cross Sections | |
|---|---|---|---|---|---|---|---|
| | | | Size | Number | | Axes 5 and 11 | Axis 8 |
| N1 | 5740 | 4.1 | #4 | 15 | 3.0 | 0.0172 | 0.0119 |
| C1 | 4910 | 3.1 | #4 | 15 | 3.0 | 0.0172 | 0.0119 |
| N2 | 5950 | 4.1 | #4 | 7 | 1.4 | 0.0081 | 0.0056 |
| C2 | 5270 | 4.7 | #4 | 7 | 1.4 | 0.0081 | 0.0056 |
| C3 | 3930 | 4.8 | #3 | 5 | 0.55 | 0.0032 | 0.0022 |
| C4 | 3930 | 4.8 | #3 | 3 | 0.33 | 0.0019 | 0.0013 |
| C5 | 3930 | 4.8 | - | | 0 | 0 | 0 |

Note: 1 psi = 0.006 895 MPa; 1 $in^2$ = 6.45 $cm^2$.

Figure 3. Location of strain gages on reinforcing bars in plan view.

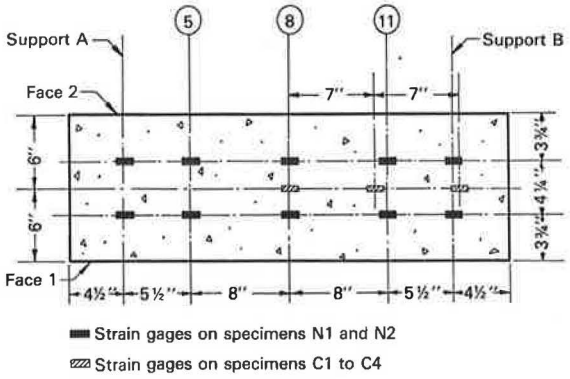


forcement of specimens consisted of 15 #4 bars for N1 and C1, 7 #4 bars for N2 and C2, 5 #5 bars for C3, and 3 #3 bars for C4 for the specimen width of 1 ft (30.5 cm). The resulting reinforcement ratio at the middle of the specimen (axis 8) varied from 0.0119 to 0.0013 and near the quarter-span (axes 5 and 11) from 0.0172 to 0.0019 (Table 1). Electrical resistance strain gages 3/8 in (0.95 cm) long were located on the reinforcing bars (see Figures 2 and 3). In specimens N1 and N2, the strain gages were located at the top and bottom of each bar, 20 gages in each specimen. In specimen N1, the gages were attached to the bars of the lower layer. In specimens C1-C4, the gages were placed at similar locations at the bottom of each bar, 3 gages in each specimen (Figure 3). The strain readings were corrected to obtain the strain and stresses at the centroid of the reinforcement in all specimens on axes 5, 8, and 11 and at the supports. Specimens N1 and N2 were equipped with strain gages placed on concrete in addition to those placed on the reinforcing. This paper includes the results of strain measurements in the steel only.

The load was applied at the top of specimens through the spherical head of 600 000-lb (2670-kN) capacity testing machines with 15 000-lb (66.7-kN) increments in the N tests and with 30 000-lb (133-kN) increments in the C tests. The test results are presented as reinforcement stress as a function of load at five locations in the N specimens, at approximately the quarter-span (axes 5 and 11), the middle span (axis 8), and the supports and at three locations in the C specimens.

## EXPERIMENTAL LOAD-STRESS CHARACTERISTICS

### Load-Stress Curves at Approximately Quarter-Span (Axes 5 and 11)

#### Specimens N1 and C1

The curves of load versus experimental stress in the reinforcement at axes 5 and 11 of specimen N1 follow the same pattern very closely from zero to failure load (see Figure 4). Both indicate elastic behavior of the concrete up to a load of about 90 kip (400 kN). Above 90 kip, the experimental stress lines begin to deviate gradually from the straight line. The first diagonal crack (shown at the left-hand side of the photograph in Figure 5) developed at a load of 135 kip (600 kN) and extended nearly half the specimen height. Further development of this crack and a new crack at the right side observed at a load of 165 kip (734 kN) are also shown in Figure 5. At 165 kip, the crack on the left side extended to about 90 percent of its final length and the crack on the right side to 60 percent of its final length. The major formation of the cracks therefore occurred between loadings of 135 and 165 kip. Correspondingly, the experimental curves exhibited a flatter pattern in this interval, indicated in Figure 4 as "major extension of diagonal cracks." This stage may be considered a transition stage, which is a stage between the elastic state of equilibrium and the cracked-elastic state of equilibrium when the steel absorbs the major portion of tensile stresses.

The new state of equilibrium of internal forces, cracked-elastic equilibrium, beginning at a load of 165 kip, is reflected by the portion of the experimental curves that follow a straight line with a slope larger than that in the transition stage but smaller than that in the elastic stage below a load of 90 kip. The left crack stopped running at 315 kip (1401 kN), as indicated in Figure 5. The experimental lines (Figure 4) indicate a flatter slope beginning with the 315-kip load. At a load of 405 kip (1801 kN), formation of a new crack starting from the existing crack at the right side was observed, beginning approximately at the 165-kip mark shown on the existing crack. The new crack extends up to the intersection of the column face (axis 7) with the sloping face of the specimen. This crack produced a sudden, explosive failure. Simultaneously, a curved crack developed at the support and there was separation of a piece behind the hooks of reinforcement. The failure occurred at stresses in the reinforcement of 38 600-39 500 psi (266-272 MPa) (see Table 2), much below the yielding stress of 45 300 psi (312 MPa). Consequently, the cause of failure was the diagonal tension (principal tensile stresses) in concrete in the direction normal to the failure crack without yielding of the steel. The experimental curve obtained from testing specimen C1 follows approximately the pattern of the experimental curves for N1 (not shown in Figure 4). Specimen C1 failed prematurely because of crushing of the specimen head at a load of 236 kip (1050 kN). Stresses for typical loads are listed in Table 2.

#### Specimens N2 and C2

The curves of load versus experimental stress at axes 5 and 11 of specimen N2 closely coincide (Figure 4). At the point indicating a load of 75 kip (333 kN), two curves of specimen N2 turn back, showing a drop in stress of about 1000 psi (6.90 MPa). The drop in stress in the steel at both axes 5 and 11 is local; the curve gradually returns to the normal pattern similar to that of specimen N1. The curve for specimen C2 indicates stresses consistently larger by 2000-3000 psi (13.8-20.7 MPa) than the stresses in specimen N2. The difference is probably due to the different arrangement of the supports. Similar higher stresses were observed in C1 for apparently the same cause.

Only two states of stresses can be clearly defined from the curves of specimens N2 and C2: the noncracked elastic and cracked elastic. The first crack, which was a diagonal crack at the right-hand side (see Figure 6), was observed in specimen N2 at the same load [135 kip (600 kN)] as in specimen N1; however, steel stress at 135 kip in specimen N2 (axis 11) was 18 200 psi (125 MPa) versus only 8200 psi (56.5 MPa) in specimen N1, which is almost exactly in proportion to the amount of reinforcement in N2. The second crack was observed in the middle of the specimen at a load of 150 kip (667 kN). A similar crack was not observed in the specimen with higher reinforcement, specimen N1. The third crack, a diagonal one, was observed at a load of 180 kip (801 kN) on the left side. Two minor sloping cracks developed at about half the distance between the

Figure 4. Stresses in reinforcement at axes 5 and 11 as a function of load.

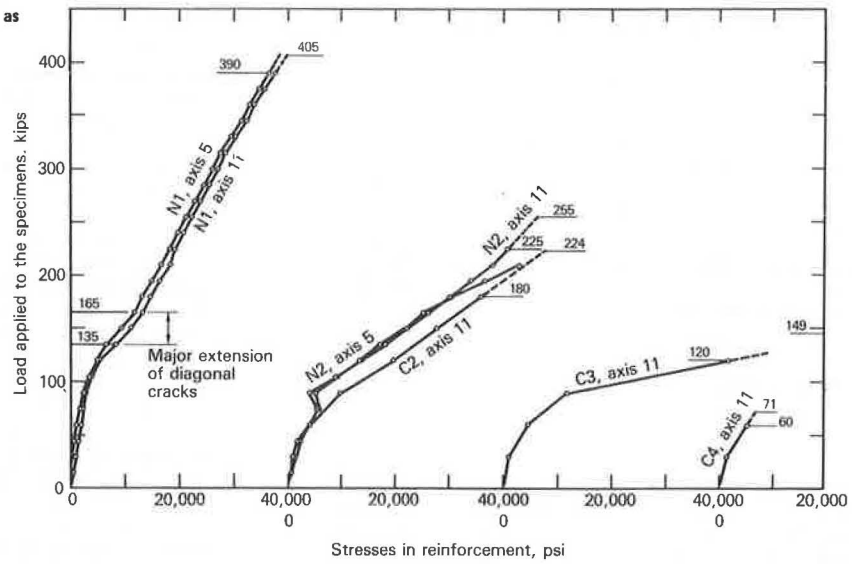


Figure 5. Specimen N1, face 2, after failure.

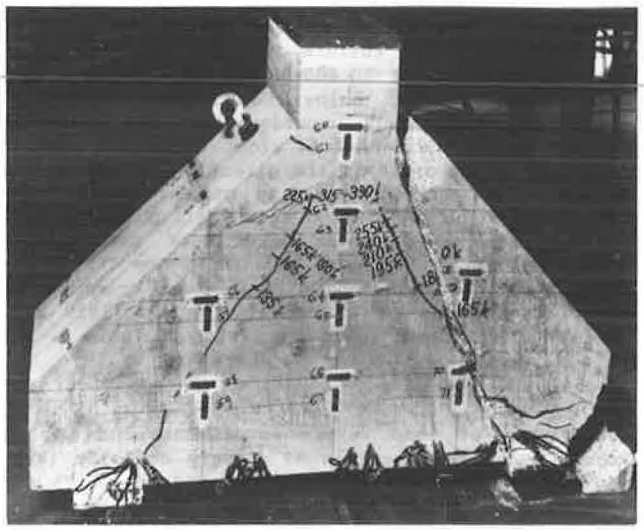

diagonal cracks, starting at the supports and the middle crack; similar cracks were also not observed in specimen N1. All five cracks were fairly symmetrically located about the center of the specimen, which may be regarded as an indication that the support conditions were symmetrical--i.e., compatible with the free support concept. A further extension of diagonal cracks was observed in both sides of the specimen at a load of 225 kip (1001 kN). The left-side crack reached the column face at axis 9, face 2, and caused the failure (Figure 6).

The appearance of the first diagonal cracks at the same 135-kip load in both specimens N1 and N2 and the extension of cracks at near the same loads in N1 and N2 (the 225-kip marks at the left side of specimens N1 and N2 are located at the same level) indicate that the amount of reinforcement does not influence the appearance and the extension of diagonal cracks. The failure of specimen N2 occurred at a load of 225 kip by a sudden, explosive failure of the concrete along the diagonal crack on the left side similar to the failure of specimen N1. A similar accompanying crack near the reinforcing bar hooks was observed as well as splitting of concrete at the hooks and at the top near the column. The failure occurred at stresses in reinforcement of 49 000 psi (338 MPa) at the middle and 46 300 psi (319 MPa) at axis 11, which were above the yield point [45 300 psi (312 MPa)]. Consequently, the cause of failure was the diagonal tension (principal tensile stresses) in concrete with simultaneous yielding of steel. The failure of specimen C2 was similar to the failure of specimen N2.

### Specimen C3

The experimental curve for specimen C3 is similar to that for specimen C2 for stresses less than 10 000 psi (69 MPa). It slopes more heavily to the right at about the 10 000-psi point as a consequence of the smaller amount of reinforcement. At a load of 90 kip (400 kN), stresses were 10 000 psi in C2 and 11 700 psi (80.7 MPa) in C3. The magnitudes of these stresses are close despite a considerable difference in the amount of reinforcement. This must be explained by the assumption that concrete resists more tension in specimen C3 with less reinforcement. The cracks that developed in specimen C3 were first observed starting from the supports as in other specimens and following a diagonal direction toward the top. A vertical crack was observed near the middle of the specimen. The experimental curve indicates that, at failure, the stress in the steel reached the yield point. The type of failure is the same as that of specimens N2 and C2: by diagonal tension in concrete with simultaneous yielding of the reinforcement.

### Specimens C4 and C5

The experimental curve of specimen C4 with low reinforcement is determined by only two points (Figure 4). An almost vertical crack developed in the specimen, starting near the middle. The same crack caused the failure at a load of 71 kip (316 kN), slightly above the second load, 60 kip (267 kN), which caused a stress of only 5300 psi (36.5 MPa) in the reinforcement. The widening of the crack caused a sudden increase of stress in the steel, which produced failure by yielding of the steel. A middle crack in specimen C3 did not produce failure whereas in C4, with less reinforcement, the vertical crack was fatal.

**Table 2. Stresses in reinforcement calculated from measured strains and corresponding loads.**

| Specimen | Stage | Load (kips) | Stress (psi 000s) Support A | Support B | Axis 5 | Axis 11 | Axis 8 |
|---|---|---|---|---|---|---|---|
| N1 | At first diagonal crack | 135 | 2.3 | 3.1 | 6.5 | 8.2 | |
| | At last recorded strain | 390 | 21.4 | 23.9 | 36.7 | 38.0 | |
| | At failure load | 405 | 23.0 | 26.0 | 38.6 | 39.5 | |
| C1 | At last recorded strain | 180 | | | | 18.7 | 18.8 |
| | At failure load | 236 | | | | | |
| N2 | At first diagonal crack | 135 | 3.0 | 4.9 | 17.2 | 18.2 | 20.3 |
| | At last recorded strain | 225 | 23.0 | 28.0 | | 40.9 | 41.5 |
| | At failure load | 255 | 28.6 | 32.5 | | 46.3 | 49.0 |
| C2 | At last recorded strain | 180 | | 25.0 | | 36.0 | 41.8 |
| | At failure load | 224 | | 37.5 | | 48.0 | 54.5 |
| C3 | At last recorded strain | 120 | | 31.2 | | 42.0 | 44.7 |
| | At failure load | 149 | | | | 67.0 | 73.0 |
| C4 | At last recorded strain | 60 | | 2.5 | | 5.3 | 12.2 |
| | At failure load | 71 | | | | 6.8 | 16.5 |

Note: 1 kip = 4.448 kN; 1 psi = 0.006 895 MPa.

**Figure 6. Specimen N2, face 1, after failure.**

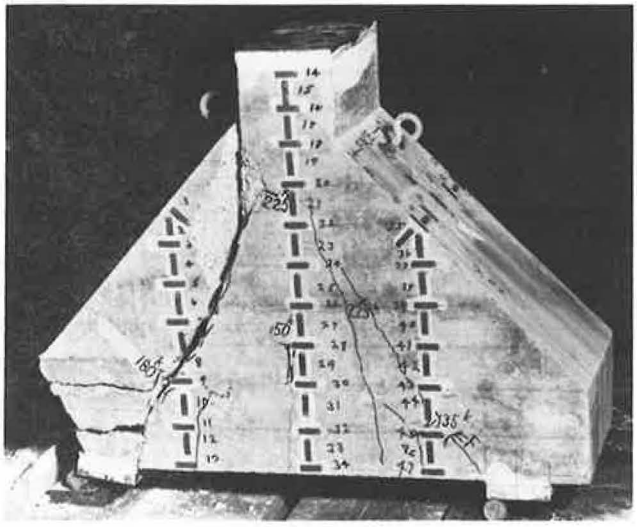

An additional specimen--C5, build with plain concrete--was tested. It failed under a load of 33 kip (147 kN), about half the load that caused the failure of specimen C4. This is an indication that even an insignificant amount of reinforcement, as in specimen C4, improves considerably the loading capacity of the specimen, a fact known by the designers of footings but not treated by the reinforced concrete design codes.

## Load-Stress Curves at Middle of Span (Axis 8)

Comparison of experimental curves (see Figures 4 and 7) obtained from strain measurements at axes 5, 8, and 11 of specimen N1 shows that the curves almost coincide. The closeness of the stresses, particularly at 165 kip (734 kN) when major cracks are formed and up to failure, indicates that stresses in the reinforcement change little along the middle portion (from axes 5 to 11) of the specimen. At the last prefailure load [390 kip (1735 kN)], stresses in the steel are 36 700, 39 400, and 38 000 psi (253, 272, and 262 MPa) at axes 5, 8, and 11, respectively; i.e., there is about 6 percent difference between the average stress in 5 and 11 and the stresses at axis 8 (Table 2). This indicates that the steel absorbs almost uniformly the horizontal component of the resultant of the principal stresses directed from the applied load toward the supports. The curves and the stresses in steel at failure for specimens N2, C1, C2, and C3 confirm the same conclusion: Stresses in the steel are nearly equal from axis 5 to axis 11 (Table 2).

## Load-Stress Curves at Supports

The general pattern of the experimental curves for specimen N1, representing stresses on supports versus loads (see Figure 8), is similar to that of the experimental curves plotted from observations of axes 5, 8, and 11. Stresses in the reinforcement at the supports, including stresses at failure, indicate values close to one-half those observed in bars in the space between axes 5 and 11 (Table 2). Stresses at failure in the reinforcement at the supports for specimens N2, C2, and C3 are larger than one-half the values of stresses in the space between axes 5 and 11.

## NOMINAL SHEAR STRESS AT FAILURE

The nominal shear stress characteristics for loads at the first diagonal crack and at failure are given in Table 3. The nominal shear stress at failure is very large, up to 2328 psi (16.0 MPa) at axis 5. This is due to the action of the reinforcement. In such structural members as deep cantilevers, the nominal shear stress cannot be used as a design criterion because it is not a measure of the shear strength (or principal tensile strength) of concrete but rather is a measure of the strength provided by tensile reinforcement.

## EQUATIONS OF EQUILIBRIUM: DESIGN OF LONGITUDINAL REINFORCEMENT

### Equations of Equilibrium

The equilibrium of a free body to the left of any vertical section passing through the left portion of the cantilever specimens will result in the equation for the reaction at the support, which is the concentrated load in the prototype ($V_u$):

$$V_u = A_s f_{su} (jd/a) \quad (1)$$

Because the stress distribution in a vertical cross section of a short cantilever with a sloping face is unknown and differs substantially from that in a long cantilever with parallel faces or in a long (shallow) beam, the equation of equilibrium, Equation 1, cannot be used directly. The arm of the

Figure 7. Stresses in reinforcement at axis 8 as a function of load.

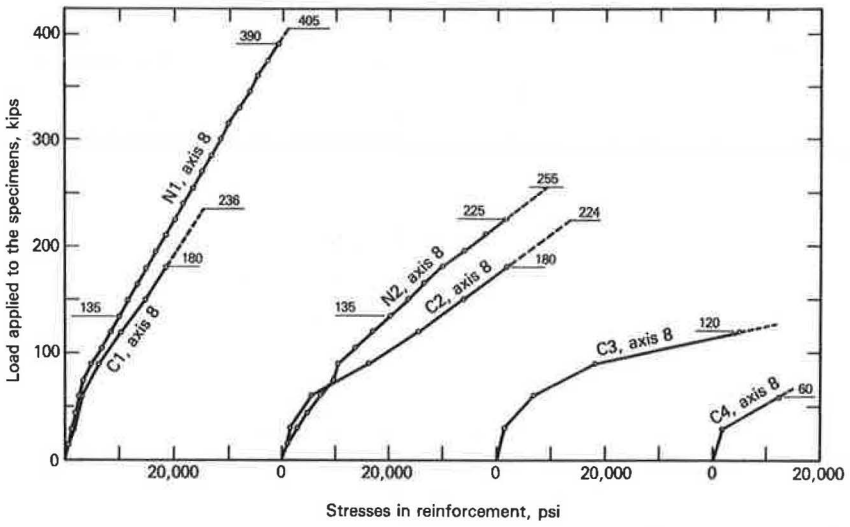


Figure 8. Stresses in reinforcement at supports as a function of load.

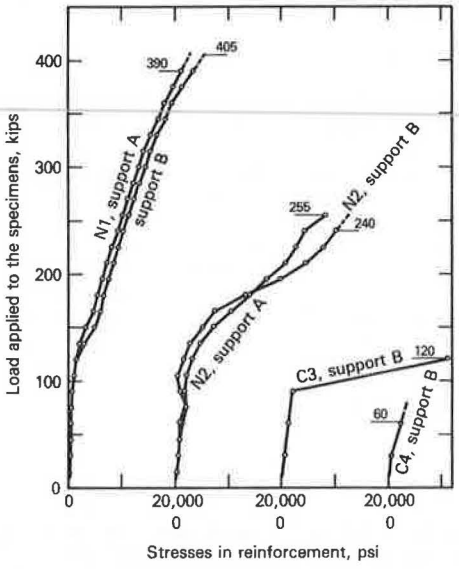


resultants of the internal normal stresses acting on a vertical section (jd) must be investigated in order to validate Equation 1 for analyzing the ultimate load ($V_u$). The stress of steel at failure ($f_{su}$) must also be assumed. Both the arm jd and the stress $f_{su}$ may be determined from the tests reported in this paper.

By rewriting Equation 1 for j,

$$j = (V/f_s A_s)(a/d) \quad (2)$$

and using 2V for the monotonic load on the specimen (V is the reaction), $f_s$, the stress from the corresponding measured strain, and the known quantities a, $A_s$, and d, the parameter j was calculated from test data and plotted versus the quantity $V/f_s A_s$ in Figure 9 for the vertical cross sections at axes 5 and 8 of specimens N1, N2, and C3. Only a portion of the available data is shown in Figure 9. Many other points that are not shown in Figure 9 would be located, if shown, exactly on the same straight lines. It is seen that the parameter j depends linearly on the quantity $V/f_s A_s$. Moreover, for specimens N1, N2, and C3, the experimental points

Table 3. Nominal shear stress characteristics.

| | Shear Stress (psi) | | | |
|---|---|---|---|---|
| | Axis 5 | | Axis 7 | |
| Specimen | At First Diagonal Crack | At Failure | At First Diagonal Crack | At Failure |
| N1 | 776 | 2328 | 577 | 1730 |
| N2 | 776 | 1466 | 577 | 1090 |
| C3 | | 856 | | 637 |
| C4 | | 408 | | 303 |
| C5 | | 190 | | 141 |

Note: 1 psi = 0.006 895 MPa.

lie on the same straight line regardless of the amount of reinforcement. Parameter j can be regarded as an index to the stress distribution in a cross section. In the beginning of the test, $j \geq 5$ (see the upper points); i.e., the resultant of normal stresses is located outside of the section, which indicates the presence of tensile stress in the cross section that corresponds to the precracked state. With increasing load 2V (and decreasing ratio $V/f_s A_s$), the parameter j decreases and reaches the value $j_F$, the value at the last observed strain prior to failure. Values of $j_F$ were calculated at sections 6 and 7 in addition to those at sections 5 and 8 (see Table 4). A graph representing the product $j_F\rho$ versus $\rho$, where $\rho$ is the reinforcing ratio, was plotted (see Figure 10). Because this plot is linear with little scatter and all four lines converge to a single point (at 0-0.12), it was possible to establish a common equation for $j_F$ as follows (for $\rho$ in percentage):

$$j_F = (0.12/\rho) + 1.36\{[(a/d) + 0.06]\} \quad (3)$$

A verification of the accuracy of Equation 3 for $\rho$ = 1 percent is given below:

| Ratio a/d | $j_F$ Calculated | $j_F$ From Graph | Error (%) |
|---|---|---|---|
| 0.38 | 0.718 | 0.72 | -0.3 |
| 0.47 | 0.841 | 0.85 | -1.2 |
| 0.54 | 0.936 | 0.87 | +1.3 |
| 0.64 | 1.072 | 1.08 | -0.7 |

The error is within 1.3 percent. This indicates

Figure 9. Internal force arm parameter (j) as a function of ratio of load to force in steel reinforcement ($V/f_sA_s$).

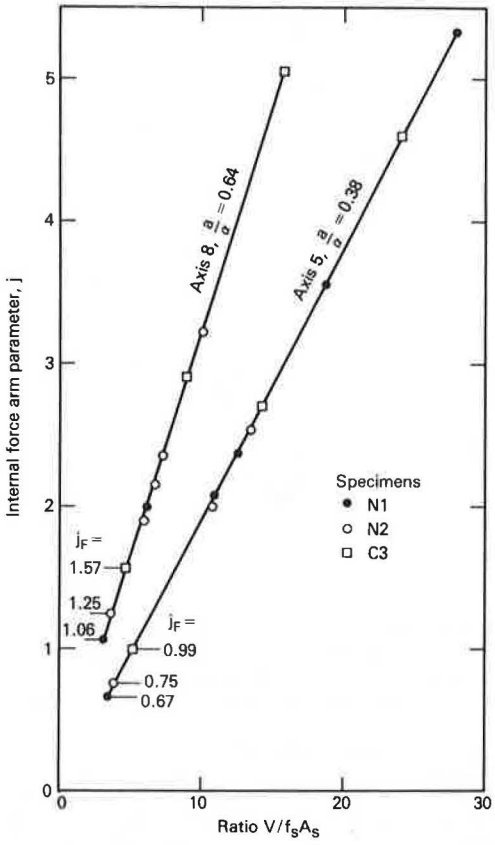


that Equation 3 provides a satisfactory method for determining the parameter $j_F$. Equation 3 provides the means for designing the reinforcement for a given load $V_u$ by using Equation 1 for the stresses in steel at the failure load. Data given in Table 2 indicate that the specimens failed at stresses in steel approximately equal to yield stress. A reduction factor of approximately 0.85 can be used. The ultimate stress corresponding to the given ultimate load will consequently be $f_{su} = 0.85f_y$.

Equation 3 can be combined with the equation of equilibrium, Equation 1, and a formula for proportioning cantilevers can be obtained as follows:

$$A_s = (V_u a - 0.0012db^2 f_{su})/[1.36f_{su}(a + 0.06d)] \quad (4)$$

for consistent units.

For a given ultimate load $V_u$ and its location determined by the shear span a, the elements of the cantilever--b, d, and $A_s$--must satisfy Equation 4. The width b must be selected to provide the space for placing the bars. Because Equation 3 is derived from experiments, the condition for compressive stress in concrete is satisfied if Equation 4 is satisfied. The nominal shear stress in concrete at a given cross section should not be considered as a design criterion (see above). Shear reinforcement is not required if the reinforcement is designed by using Equation 4. Because Equations 1-4 are derived based on satisfying the laws of statics, the principle of superposition can be applied when they are used; i.e., any number of concentrated loads from girders resting on a bridge pier may be included in this analysis.

## Design of Reinforcement

An example of a design is provided: For an ultimate load $V_u$ = 600 kip (2669 kN) located at a = 5.0 ft (152 cm) from the column, design the cross section at the column. Use steel $f_y$ = 45 ksi (310 MPa), use stress at failure $f_{su}$ = 0.85 x 45 = 38.25 ksi (264 MPa), and assume a cross section with b = 24 in (61 cm) and d = 48 in (122 cm). From Equation 4, the necessary reinforcement will be as follows:

$$A_s = [600 \times 5 \times 12 - 0.0012 \times 48 \times (24)^2 \times 38.25] \div [1.36 \times 38.25(5 \times 12 + 0.06 \times 48)] = 10.62 \text{ in}^2 (68.5 \text{ cm}^2)$$

The corresponding value for $j_F$ for this analysis by Equation 3 is $j_F$ = 1.92. A similar design for a shallow beam determined by using the ultimate load method results in substantially larger reinforcement. By using "Witney's block" for compressive stresses and $0.85f'_c$ stress (7, p. 50), the reinforcement is $A_s$ = 26.8 in² (173 cm²) with j (same as $j_F$ above) = 0.732.

## Geometry

The cantilevers were tested by using specimens of particular geometry (Figures 1-3). However, the essential geometric characteristic that determines the behavior of this type of structure is the shear-span-to-depth ratio, a/d. If the slope of the lower surface of a bridge pier or the height at the end of the cantilever is different from those of the tested specimens but the essential characteristic, a/d, remains the same at a given cross section, the characteristic of the section at failure ($j_F$) must remain essentially the same. However, testing is desirable to confirm the applicability of the method to other cantilever shapes, particularly for bridge piers with a steeper lower surface--i.e., with larger depth-to-span ratio (d/a).

The above argument does not apply, however, to such structural elements as corbels (brackets). Because corbels (brackets) projecting from columns or walls have substantially different geometry near the column or wall face and consequently a different stress pattern near the support than deep cantilevers, Equations 3 and 4 may not provide sufficiently accurate results if applied to corbels. This conclusion follows from several trial calculations based on PCA test data (1).

## INVESTIGATION OF NORMAL STRESS DISTRIBUTIONS AT A CROSS SECTION

A study of $j_F$ values from Figure 9 and Table 4 indicates that at lower reinforcement parameter $j_F$ is larger. When $j_F > 1$, the resultant of the normal stress in the cross section is located outside the cross section. This indicates that tension in the concrete must exist prior to failure. On the other hand, when the ratio $V/f_sA_s$ decreases (Figure 9), the parameter j decreases. The parameter j is greater than 5 at the beginning of the test at low loads, when the precracked condition exists; it gradually drops to the value $j_F$ indicated in Figure 9.

At the prefailure conditions concrete still resists tension, apparently at the lower portion of the cross sections, despite the fact that major cracks develop at the support. The hypothesis that concrete still resists tension at the prefailure stage (indicated by a large value of $j_F$) may be supported also by the fact that the concrete does not exhibit cracks at the reinforcing bars between the supports if a sufficiently large amount of reinforcement is provided (specimen N1). This also means that the bond between the bars and the concrete is not broken and therefore concrete participates in resisting tension in addition to the resis-

**Table 4. Parameter $j_F$ at last recorded strain determining location ($j_F d$) of resultant of normal stresses in concrete and corresponding $\rho$.**

| Test | Load 2V on Specimen at Last Recorded Strain (kips) | Section at Axis No. 5 | | 6 | | 7 | | 8 | |
|---|---|---|---|---|---|---|---|---|---|
| | | $j_F$ | $\rho$ (%) | $j_F$ | $\rho$ (%) | $j_F$ | $\rho$ (%) | $j_F$ | $\rho$ (%) |
| N1 | 390 | 0.67 | 1.72 | 0.81 | 1.47 | 1.91 | 1.28 | 1.06 | 1.19 |
| N2 | 225 | 0.75 | 0.81 | 0.92 | 0.69 | 0.97 | 0.60 | 1.25 | 0.55 |
| C3 | 120 | 0.99 | 0.32 | 1.20 | 0.27 | 1.35 | 0.24 | 1.57 | 0.22 |

Note: Shear span/depth ratio (a/d) = 0.38, 0.47, 0.54, and 0.64 for sections 5, 6, 7, and 8, respectively.

**Figure 10. Parameter $j_F\rho$ as a function of the reinforcement ratio, $\rho$, and arm-to-depth ratio a/d.**

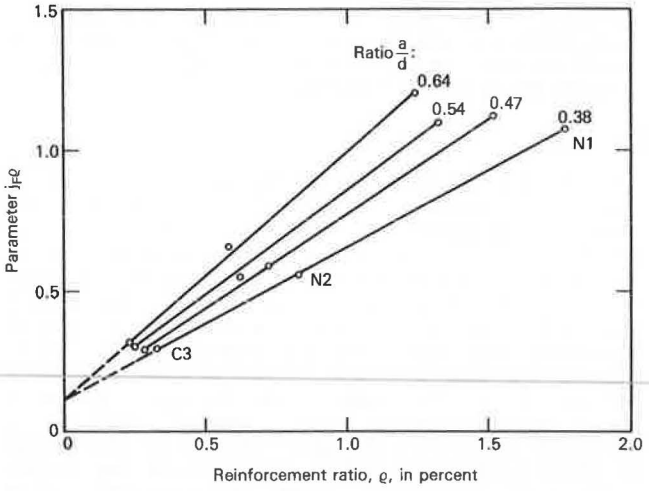


**Figure 11. Normal stress distribution in concrete in specimens N1 and N2 at last observed strain at axis 7 prior to failure.**

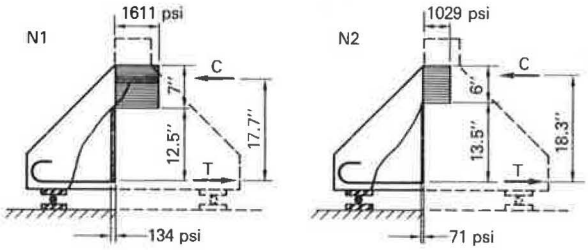


tance of the bars. In specimen N2 vertical cracks developed, so the participation of concrete in absorbing tension stress is not so obvious for this specimen.

An analysis done for specimens N1 and N2 by using the actual values of $j_F$ results in the normal stress distribution diagrams shown in Figure 11a, b. This analysis assumes the neutral plane at the intersection of the major crack with the cross section at axis 7. Observed strain, given load, reinforcement data, and the magnitude of the parameter $j_F$ (Equation 3) are used. The compressive stress block is assumed to be rectangular. If the rectangular compressive stress block is used, tension stress below the neutral plane must be present to satisfy the condition of equilibrium. Calculated tension stresses are shown in Figure 11. If a parabolic stress distribution or a triangular compressive stress diagram were assumed, the tension stress below the neutral plane necessary for equilibrium would still exist but would be smaller. If a similar analysis were made at axis 8 (instead of axis 7) with $j_F$ = 1.06 (for N1) and 1.25 (for N2), the tension necessary for equilibrium would be larger than in the example analyzed for axis 7 because the resultant C of stresses in concrete is located at axis 8 outside the cross section ($j_F > 1$) (Table 4). The magnitudes of the stresses calculated for specimens N1 and N2 are shown in Figure 11.

## CONCLUSION

Tested deep reinforced concrete cantilevers exhibit substantially higher resistance to applied load than that determined by conventional methods of analysis using the ultimate load or working stress method. A study based on equilibrium of tested specimens provided a method for determining the arm of the resultant of normal stresses in concrete in a vertical cross section as a function of depth-to-span ratio and reinforcement ratio. A general equation for analyzing the arm of this resultant is presented. In turn, this equation provides the means for designing the reinforcement to satisfy conditions of equilibrium prior to failure. Conditions for compression of concrete are satisfied by using this equation. It has been found that nominal shear stresses at vertical cross sections are very large, much above the shear (principal tension) strength of concrete. This is because the horizontal reinforcement provides shearing strength to the structure. For this reason, nominal shear stress should not be used as a criterion for the design. The true distribution of normal stresses prior to failure in vertical cross sections is still unknown, although the equilibrium study indicated that tension in concrete exists and contributes to the overall resistance of deep cantilevers. This in part explains their higher resistance to the applied load compared with that predicted by conventional methods of analysis.

## ACKNOWLEDGMENT

The testing at Case Institute of Technology was performed under my supervision by J. Schleich, who was then a graduate student. The testing at the National Bureau of Standards was performed under my direction with the participation of R.G. Mathey and L. Catanio. I express my great appreciation to them.

## REFERENCES

1. L.B. Kriz and C.M. Raths. Connections in Precast Concrete Structures: Strength of Corbels. Journal of Prestressed Concrete Institute, Vol. 10, No. 1, Feb. 1965, pp. 16-61.
2. Joint ASCE-ACI Task Committee 426 on Shear and Diagonal Tension. The Shear Strength of Reinforced Concrete Members. Journal of Structural Division, ASCE, No. ST6, Proc. Paper 9791, June 1973, pp. 1091-1187.
3. H. Niedenhoff. Untersuchungen ueber das Tragverhalten von Konsolen und kurzen Kragarmen. Karlsruhe Tech. Univ., Karlsruhe, Federal Republic of Germany, dissertation, 1961.

4. G.U. Franz and H. Niedenhoff. Die Bewehrung von Konsolen und gedrungenen Balken. Beton und Stahlbeton 5, 1963, pp. 112-120.
5. A.H. Mattock, K.C. Chen, and K. Soongswang. The Behavior of Reinforced Concrete Corbels. Journal of Prestressed Concrete Institute, Vol. 21, No. 2, March-April 1976, pp. 52-77.
6. A.H. Mattock. Design Proposals for Reinforced Concrete Corbels. Journal of Prestressed Concrete Institute, Vol. 21, No. 3, May-June 1976, pp. 18-42.
7. P.M. Fergusson. Reinforced Concrete Fundamentals, 4th ed. Wiley, New York, 1979, 724 pp.

*Publication of this paper sponsored by Committee on Concrete Bridges.*

# Study of Cracking of Composite Deck Bridge on I-75 over Peace River

CLIFFORD O. HAYS, JR., FERNANDO E. FAGUNDO, AND ERIC C. CALLIS

**Observed cracking on the Peace River Bridge on Interstate 75 near Punta Gorda, Florida, caused concern about the possibility of high maintenance cost and the structural adequacy of the bridge system. The deck system consists of precast panels resting on soft fiberboard, which serve as formwork for the road surface and later aid in carrying the traffic loads. An investigation has been completed that involved testing of the Peace River Bridge, testing of the FL-776 Bridge (a nearby structure of similar construction), analytic modeling using the finite element method, and limited laboratory testing of beam specimens. The investigation indicates that although the Peace River Bridge is adequate to carry normal traffic, the shear stresses in the bridge deck are substantially higher than those of deck systems that have positive bearing at the ends of the panels. Further experimental studies are under way to determine the shear fatigue life of the bridge. The causes of cracking and separation at the ends of the panels are identified as differential shrinkage and creep due to prestress forces. Recommendations for future construction projects are made.**

Rising costs of formwork, materials, and labor have greatly increased the cost of reinforced concrete bridges constructed with conventional field forming techniques. Construction techniques that reduce the amount of forming done under field conditions increase the economy of the bridge. Prefabricated prestressed girders have been in common use in bridges for approximately 30 years. Precast stay-in-place forms of concrete and steel replaced wooden forms in recent years and eventually led to the development of precast composite deck panels. Composite deck panel bridges contain precast prestressed panels that span between bridge girders and support the cast-in-place topping, eliminating most of the field formwork. Research in Florida, Pennsylvania, and Texas led to their widespread acceptance and incorporation into the American Association of State Highway and Transportation Officials (AASHTO) specifications (1). Figure 1 shows typical composite bridge panel construction, as built in Florida, prior to this research.

Recent research in Florida (2) and Louisiana (3) dealt with full-span form panels that span directly between piers without using prestressed girders. Additional research on deck panels was recently completed in Texas (4). Although there are significant differences in these two types of construction, they both exhibit more regular cracking patterns than bridges with reinforced concrete decks constructed by using conventional forms. The combination of (a) shrinkage due to placing a thin layer of fresh concrete on top of a deck panel that has already undergone a major portion of its shrinkage and (b) vertical joints between panels and cast-in-place concrete in regions of high stress (due to traffic) will cause cracking and the cracking will follow a regular pattern. However, extensive research and experience have shown that these systems can be safely used in bridge construction.

The Peace River Bridge on I-75 near Punta Gorda, Florida, was constructed with prestressed girders and composite deck panels. During the construction of the bridge, an unusually large number of cracks were observed in the deck. As pointed out earlier, some cracking is inherent in this type of construction, but the extensive early cracking that was observed caused concern about the possibility of excessively high maintenance costs due to deterioration of the deck with time.

Preliminary studies of the plans for the Peace River Bridge indicated one major difference from details used in other states. On the Peace River Bridge, and other bridge work in Florida, the precast panels are supported, as shown in Figure 1, by fiberboard so that the panels do not have positive bearing on the girders. One series of the Florida panel tests (5) was made without positive bearing for the panels, and satisfactory performance of the panels was observed. However, these test panels had prestressed strands that extended a short distance into the cast-in-place concrete. In addition, these laboratory test specimens were not exposed to temperature, creep, and shrinkage stresses, which aggravate the cracking near the end of the panels under field conditions.

The panels are designed to act compositely with the cast-in-place concrete in resisting live loads and are assumed to act as a continuous slab with negative moment developed in the slab over the girders. The ability of the panels to transfer shear across their ends and provide continuity was questioned due to the observed cracking. Prior research concentrated heavily on demonstrating that adequate bond could be developed between the top of the panels and the cast-in-place topping. Only minimal attention was given to the bond between the end of the panels and the cast-in-place concrete over the girders. The exact mechanism of the shear transfer and the degree of continuity in this region of interfaces between various concretes with creep, shrinkage, and temperature cracks is difficult to predict with any degree of certainty. Thus, a thorough investigation of the Peace River Bridge was warranted.